CHARACTERIZATION OF VARIOUS FLUIDS IN CYLINDERS FROM DOLPHIN SONAR DATA IN THE INTERVAL DOMAIN

Claudia Lainscsek and Irina Gorodnitsky
Cognitive Science Department,
University of California at San Diego,
La Jolla, CA 92093-0515, USA,
e-mail: clainscsek@ucsd.edu, igorodni@cogsci.ucsd.edu

Abstract: ***An algorithm to map temporal signals into sequences of timing patterns is introduced and applied to the analysis of dolphin sonar data collected during a target discrimination task. A parallel can be drawn between this algorithm and the biological auditory system which encodes sensory information in the timing patterns of neural spike trains. The information in this case is carried in the interval lengths between adjacent spikes hence we term this representation an Interval Domain Representation (IDR). A classification feature space is defined in this domain and used to analyze the returning echoes in dolphin data. We show that the dynamical classifier is able to discriminate with high confidence cylinders filled with four different fluid types used in the experiment. The potential applications of this research include improved target discrimination and a more general classification of complex acoustic data, including biologic data. The research may also provide clues to understanding the complexities underlying dolphin sonar discrimination capabilities.***

I. Introduction

The auditory system encodes incoming acoustic signals in the timing sequences of spike trains originating in the inner ear, meaning that the signal information is carried by the intervals between the adjacent spikes. This interval domain representation is fundamentally different from time or frequency domain representations used in signal processing. How a band-pass signal can be represented by interval information, as opposed to Nyquist rate amplitude sampling, is not understood to date. This representation, however, is thought to be the key to the auditory system ability to encode signals that are broadband or have time varying spectra.

We have recently developed a transformation from the temporal domain to the interval domain. We have also shown the relationship between the timing intervals and the frequencies contained in a signal [1]. The resulting representation is an expansion of the data derivative in terms of linear and non-linear functions containing the interval lengths as the parameter. Equivalently, the representation is a Delay Differential Equation (DDE). The timing intervals in the auditory encoding correspond to what are called the time delays in the DDEs. We also use the term delays through out the paper to refer to the encoding interval.

The interval encoding representation is used in the paper to analyze the returning echoes from dolphin sonar data collected during a classification task. The task involves discriminating four types of fluids in cylinders. A feature set in the interval representation is derived and is shown to be sufficient for the classification of the four fluids.

DDE analysis of dolphin sonar data has been done in [2] with the exception that only the outgoing sonar pulses were analyzed and the delays were fixed to be constant. The inspiration for DDE application was not biologically based and constant delays produces very different results. For example, this approach cannot classify the fluids from the data presented here.

II. Interval Domain Representation

Here we give a very abbreviated introduction to IDR.

Given a one dimensional vector $x(t)$ one can construct a representation using time-delayed vectors as $\mathbf{X}(t)=\{x(t),x(t-\tau_1),\ldots,x(t-\tau_{d-1})\}$ according to the embedding theory developed by Takens [3], Packard et al. [4], and Sauer et al. [5]. The representation is an embedding with a variable delay τ_i, $i<d$. The importance of this construct is its diffeomorphism to the original space for a sufficiently large embedding dimension d so that topological properties are preserved under relatively loose restrictions. This means we can express the temporal evolution of $x(t)$ in the embedding space, i.e.

$$\frac{dx(t)}{dt}=F\left(x(t),x(t-\tau_1),\ldots,x(t-\tau_{d-1})\right) \tag{1}$$

which is a Delay Differential Equation (DDE) with non-uniform delays. Eq. (1) gives the connection between the time domain and the interval domain. DDEs are known for being able to express complex system behaviors. Of particular interest here, as we show in [1], is the fact that the variable frequencies can be represented directly in the IDR, which is not possible in the Fourier Domain.

In order to find the representation Eq. (1), one must determine the model functions

$$F(x(t), x(t-\tau_1), \ldots, x(t-\tau_d))$$

from the data but this problem is ill-posed and very difficult computationally. It requires one to assume some general expansion form for the model $F(x(t), x(t-\tau_1), \ldots, x(t-\tau_d))$ and then to fit the coefficients in the general expansion at successive observation points t. Polynomial expansions are the most practical in this case because they reduce the problem to having a linear dependence in the unknown coefficients which can be estimated directly via a least-squares fit.

III. Principles of Detection and Classification in the interval domain

To estimate the model functions in Eq. (1) from the data it is necessary to reduce the degrees of freedom in Eq. (1) to make it tractable. Hence, we assume a low order model approximation to Eq. (1) which is crucial in making this approach practical. In general, nonlinear models are notoriously sensitive to small changes in the data. Detection and classification require that the classification space captures the essential features of the signals that are sufficient to separate them. At the same time, robust estimation can be achieved by providing a 'loose' fit between the model and the data, that is to fit data to within some uncertainty using a low order model approximation. This is nothing else than the regularization principle used in Linear Estimation.

For a low-order approximation, we select the leading terms from Eq. (1), which are the linear and a few low order non-linear terms. It can be written as

$$\dot{x} = \sum_k a_k \, x_{\tau_i}^{l} x_{\tau_j}^{m} \tag{2}$$

where $x_{\tau_i} = x(t-\tau_i)$ and $i, j, l, m \in \mathrm{N}_0$, and x_{τ_i} permits zero values. In our analysis we select the nonlinear terms with up to the third order non-linearities only. The classification space for this construct is $\{a_k, \tau_i\}$, $i = 0,1,2$, that can be used to quantify the differences between signal classes.

IV. Dolphin data

The IDR is used here to analyze dolphin sonar data collected during a target classification task. The data was provided by the Biosonar Program Group at SPAWAR Systems Center in San Diego. In the experiment the same task is performed on five different days by the same dolphin. The dolphin is presented with targets which are SIGG fuel bottles made of spun aluminum and filled with four types of fluids: fresh water, karo syrup, glycerol, and saline solution. To classify the fluids, the dolphin acoustically images the fluids by producing short outgoing pulses that ensonify the targets. The returning "echo" is the complex backscatter from the suspended target. The dolphin classifies the material contained in the target using the "echo" structure.

The data analyzed here were digitized at 500 kHz, with 256 points per echo waveform, stored as signed 16-bit integers providing 12-bit accuracy. The full-scale voltage range was +/- 10 V. The system gain and filtering remained constant throughout the data collection.

V. Model- and Delay- selection for the Dolphin data

The echo data is transformed to the IDR as follows. We consider low order models derived from Eq. (2) with a small number of terms and up to cubic non-linearities. From our experience with representing acoustic data we expect two-delay models to provide a sufficiently good classifier for the given data. We use a Genetic Algorithm (GA) to estimate the best low order model from Eq. (2) and the associated coefficients and delays. The GA is run in two steps, the delay-selection and the model-selection step. The GA depends on four modeling parameters, i) the number of delays, N_τ, ii) the maximal number of coefficients in the models, N_c, iii) the order of nonlinearity, O_n, and iv) the initial population size, N_p. A first set of delays and the initial population of models are generated with a random number generator. The GA is applied to model-selection until the residual does not change for 5 iteration steps. The best model, with the smallest average least square, is selected and, starting from the initial population of delays, the GA is applied to delay-selection. The process is then repeated from the beginning using the best models of former runs. The alternative run of the two codes is terminated when no change in the residual is observed in both steps of the GA. The resulting model has the smallest average least square error across all data sets.

Several adaptations may be needed to extract a DDE model from sampled data. Since the delays are integers, we found that the present data needed to be upsampled by a factor of 10 in order to have fine enough interval resolution to reveal material structure features in the echoes. The upsampling has three advantages: i) The upsampled data are smoother and therefore the derivatives can be estimates more accurately. ii)The estimated model parameters are more consistent over the data set. iii) Non-integer delays can be simulated by this method.

Following these procedures we find the best DDE on average to be

$$\dot{x} = a_1 \, x_{\tau_1} + a_2 \, x_{\tau_2} + a_3 \, x_{\tau_1} \, x_{\tau_2} \tag{3}$$

where $x = x(t)$ is the upsampled time-series and $x_{\tau_i} = x(t - \tau_i)$ with $i = 1,2$ are the delayed versions of x.

The model in Eq. (3) was found by optimizing across a set of models in the minimum least square sense. The model coefficients can be re-estimated better by optimizing over coefficient space of this model. With the first pass of the GA we find that for all targets the first optimized delay is in the range between 11 and 13 and the optimal value for second delay varies between 100 and 600, depending on the fluid. Thus we repeat the optimization over the coefficient space while restricting the first delay to 11 and the second delay to a range between 100 and 600.

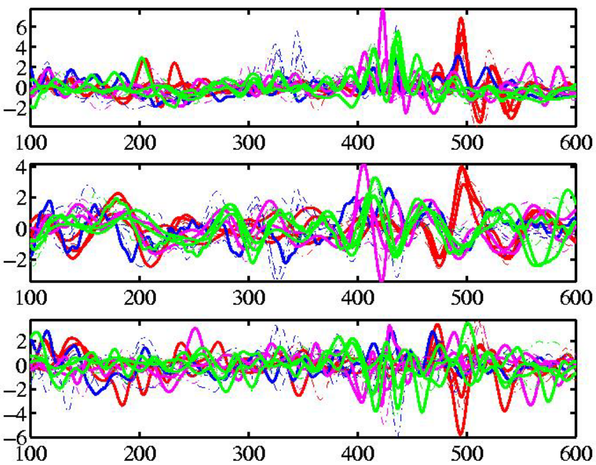

Figure 1: Plot of the estimated coefficients a_1, a_2, a_3 as a function of the second delay τ_2 in the selected range. The colors are: glycerol is red, saline is blue, karo is green, and fresh water is turquoise.

Fig.1 shows the mean of the obtained coefficients a_1, a_2, a_3 as a function of the second delay τ_2. Each color represents a different fluid and the different lines of the same color represent different trials. From Fig. 1 one can see that the different fluids have very distinctive model parameters that become synchronized across the trials and increase in value in different τ_2 ranges. We identify four regions where this is observed for one or more fluids. For example, in the case of glycerol, the coefficients become distinct and synchronized for all five trials when τ_2 is in the range approximately between 450 and 525.

The values of the model coefficients, a_1 versus a_2, are plotted for these four regions in Fig. 2. For each region we select and plot the a_1 / a_2 values taken from this region. The τ_2 values for which the points are plotted are shown at the top of each plot. Thus in Fig 2(a) we plot the four a_1 / a_2 values, one for each τ_2 point within the 493 and 496 range (four values) for each fluid type. The rest of the τ_2 ranges contain 6 points. The values for each trial are clustered together and are easily identified. We draw a line to show the distinct separation of each fluid from the rest of targets in the classification space. It is clear that each fluid has a unique feature set $\{\tau_2, a_1, a_2\}$ associated with it for the optimal τ_1 value.

The small circles in Fig. 2 indicate cases where the dolphin was wrong in its classification. In most of those cases our algorithm classified the fluids correctly in each τ_2 range, except in two instances involving karo and fresh water. These two media overlap for the feature coefficient values we selected in one out of five trials. Significatly, however, this erroneous classification involves a different trial in the two τ_2 ranges (421:417 and 325:330). Thus the discrepancy in the classification of the two fluids in the two τ_2 ranges is identifiable from the given coefficients, so that the fluids could be tested further to resolve the ambiguity.

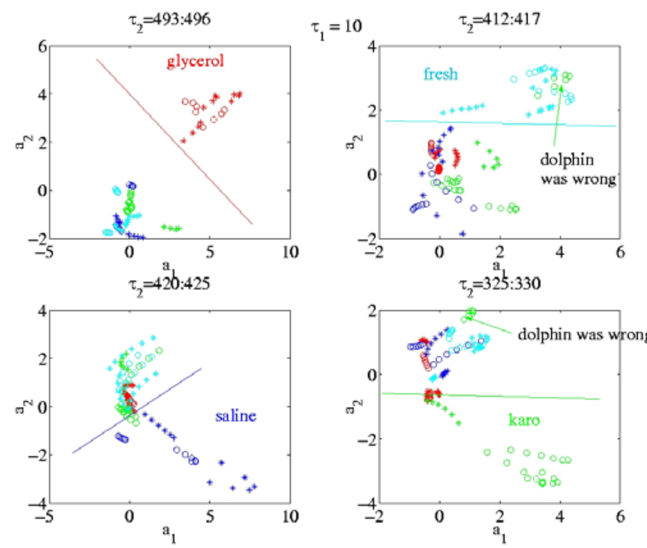

Figure 2: Projections of the coefficients onto the $a_{1,2}$-plane for selected τ_2 ranges. "✳" indicates trials where the dolphin was correct and "**O**" indicates where the dolphin was wrong. The colors are: glycerol is red, saline is blue, karo is green, and fresh water is turquoise.

VI. Discussion

The paper presents a first investigative attempt to understand how biologically inspired interval domain representation can be used for acoustic classification. Many improvements on the procedure can be made. Selecting only the echoes that produce a significantly lower residual would make the coefficient estimates more stable. Such selection is also compelling due to the fact that the dolphin produces many clicks presumably to select the ones that produce consistent estimates. The model used here may also be improved by searching over a bigger set of models and by refining our model-delay iterative optimization search. Another improvement would be to optimizing the number of points from which the derivative is computed.

VII. References

[1] Manuscript in preparation

[2] M. Kremliovsky, J. Kadtke M. Inchiosa, and P. Moore, "Characterization of dolphin acoustic echo-location data using a dynamical classification method," Int. J. of Bifurcations and Chaos, vol. 8, p 813, 1998.

[3] F. Takens, "Detecting Strange Attractors in Turbulence," Lecture Notes in Mathematics, vol. 898, p. 366, 1981.

[4] N.H. Packard, J.P. Crutchfield, J.D. Farmer, and R.S. Shaw, "Geometry from a Time Series," Phys. Rev. Lett. Vol. 45, p. 712, 1980.

[5] T. Sauer, J.A. Yorke, and M. Casdagli, "Embedology," Journal of Statistical Physics, vol. 579, p. 65, 1991.